K-7-5

Extended Abstracts of the 2009 International Conference on Solid State Devices and Materials, Sendai, 2009, pp1392-1393

Spin-transfer switching and enhanced thermal stability of magnetic tunnel junctions with CoFeB/Ru/CoFeB ferromagnetically-coupled free layer

Hitoshi Kubota, Satoshi Yakata, Akio Fukushima, Kay Yakushiji, Takayuki Seki, Shinji Yuasa, Koji Ando

National Institute of Advanced Industrial Science and Technology (AIST), Tsukuba Central 2, 1-1-1, Umezono, Tsukuba 305-8568, Japan

Phone: +81-29-861-3949 E-mail: hit-kubota@aist.go.jp

1. Introduction

Important issues for the development of Spin-RAM [1] are low switching current (I_c), high thermal stability ($\varDelta$) and large magnetoresistance (MR) ratio. I_c should be smaller than a maximum current of a path transistor. $\varDelta_0$, defined as $\varDelta_0 = K_u V/k_B T$ (K_u, V, k_B and T are uniaxial magnetic anisotropy, volume, Boltzman constant and temperature, respectively), should be larger than 40 to guarantee a long retention time of 10 years by suppressing thermal fluctuation in a nanomagnet. The large MR ratio is required to discriminate precisely low and high resistance states those distribute around mean values in many cells.

To satisfy above requirements simultaneously, two approaches are under way: The first one is the development of magnetic tunnel junctions (MTJs) with perpendicular magnetic anisotropy (PMA), which is expected to exhibit low I_c and high $\varDelta$ [2]. In this approach the synthesis of new magnetic materials with PMA is a key to success. The second one is the development of advanced in-plane magnetized MTJs. Ordinary in-plane MTJs (e.g. CoFeB/MgO/CoFeB) [3] have shown large MR ratios but I_c and $\varDelta$ have been in trade-off relation, thus, it seems impossible to satisfy the requirements. Hayakawa and co-workers reported low I_c (~5 MA/cm^2) and high $\varDelta$ (~90) using antiferromagnetically (AF)-coupled CoFeB/Ru/CoFeB free layers [4, 5]. Compared with a single 4-nm-thick CoFeB layer, I_c was actually half in the AF-coupled CoFeB(2 nm)/Ru/CoFeB(2 nm) case. However, the mechanism of high $\varDelta$ remained unclear.

In this report, we studied systematically spin-transfer switching of the CoFeB/Ru/CoFeB coupled free layer systems. The results indicate that $\varDelta$ can be more enhanced in ferromagnetically (F)-coupled free layer system. It is confirmed that we can control I_c and $\varDelta$ independently using the coupled free layer system. Physical mechanism of the enhanced $\varDelta$ is also discussed.

2. Sample preparation

Using a UHV magnetron sputtering machine Si substrate/buffer/Pt-Mn 15 nm/Co-Fe 2.5 nm/Ru 0.85 nm/$Co_{60}Fe_{20}B_{20}$ 3 nm/MgO 1 nm/ free layer /Ta/Ru multilayer films were prepared. Layer structures of the free layers are shown in Figs. 1: (A) AF-coupled $Co_{60}Fe_{20}B_{20}$ 2 nm/Ru 1.1 nm/ $Co_{60}Fe_{20}B_{20}$ 2 nm film, (B) F-coupled $Co_{60}Fe_{20}B_{20}$ 2 nm/Ru 1.5 nm/ $Co_{60}Fe_{20}B_{20}$ 2, and (C) F-coupled $Co_{60}Fe_{20}B_{20}$ 2 nm/Ru 1.5 nm/ $Co_{60}Fe_{20}B_{20}$ 4 nm film. Samples were microstructured into 80 nm ×140 nm elliptical shape using electron beam lithography combined with Ar ion etching. The samples were annealed at 300°C for 1 hour by applying 1 T magnetic field.

3. Tunnel magnetoresistance

Resistance (R)-magnetic field (H) curves were measured using a lock-in amplifier. The MR ratio is defined as $(R_{AP}-R_P)/R_P \times 100(\%)$, where R_{AP} (R_P) is a tunnel resistance when the magnetizations adjacent to the MgO layer are aligned anti-parallel (AP) (parallel (P)). Figures 2 show typical R-H loops of Sample A-C. Every loop shows sharp transitions between high and low resistance states. Center fields of the loops shift slightly to positive (H_{shift}). The MR ratios are about 130% in Sample A and B and slightly smaller in Sample C.

4. Spin-transfer switching

Spin-transfer switching was observed by applying a pulse current (I) (200 ms constant) with an external magnetic field (H_{ext}). Switching time (t_{sw}) was determined from resistance change as shown in the inset of Fig. 3(a). The measurement was repeated many times by changing I and H_{ext}.

When pulse duration is long (> 10 ns) magnetization switching induced by the spin-transfer is thermally activated. [6] In this regime, switching probability (P_{sw}) is expressed as

$$P_{sw} = 1-\exp[-(t_{sw}/\tau_0)\exp(-\varDelta_2)], \quad (1)$$

$$\varDelta_2 = \varDelta_1(1-H_{eff}/H_{c0})^2, \quad (2)$$

$$\varDelta_1 = \varDelta_0(1-I/I_{c0}), \quad (3)$$

where τ_0, H_{eff}, H_{c0}, $\varDelta_0$, I_{c0} are inverse of attempt frequency (1 ns), effective magnetic field, coercive field at 0 K, intrinsic thermal stability and intrinsic switching current, respectively. I_{c0} and $\varDelta_0$ are also important characteristics in device operation.

Figure 3(a) shows an example of t_{sw} dependence of P_{sw} obtained under constant I and H_{ext}, which is well reproduced by eq. 1. Figure 3(b) shows H_{ext} dependence of $\varDelta_2$ for I = ±0.7 mA, which are well reproduced by eq. 2. An intersection of the curve with a vertical line at H_{eff} (=H_{ext} - H_{shift})=0 gives a value of $\varDelta_1$. I dependence of $\varDelta_1$ for Sample A-C are shown in Figs. 4(a)-(c), respectively. Lines represent theoretical fit using eq. 3. The y- and x-intercepts represent $\varDelta_0$ and I_{c0} values, respectively.

5. Discussion

MR and switching properties of Sample A-C are summarized in Table 1. The values are averaged over some identical samples. J_{c0}^{ave}, which is switching current density defined by $(1/2)(I_{c0}^{AP\ to\ P} + I_{c0}^{AP\ to\ AP})$/(junction area), is almost same in the three types of the samples. This result is in contradiction to the previous result [4]. H_{c0}^{ave} value of Sample A is larger than that of Sample B. However, the large value does not correspond to the enhancement of thermal stability in this system because the AF arrangement of the magnetizations reduces Zeeman energy. In a distorted cell such as our present samples, shape magnetic anisotropy that gives a potential during magnetization reversal is responsible dominantly to the thermal stability. Therefore, the AF arrangement reduces the potential in Sample A remarkably. Interestingly, Sample B shows smaller H_{c0}, but larger Δ_0^{ave}. The F arrangement of the magnetizations enhances the energy potential, resulting in higher bi-stability of the magnetizations. Sample C shows more enhanced Δ_0^{ave} nearly 300, which is comparable to perpendicularly magnetized systems. The enhanced shape anisotropy energy by the thick CoFeB 4 nm film gives highly stable magnetizations with keeping J_{c0} constant.

6. Conclusions

We have investigated systematically spin-transfer switching current and thermal stability in CoFeB/Ru/CoFeB coupled-free layers. The thermal stability factor is dominated by the shape magnetic anisotropy, which is more enhanced in the F-coupled free layers than in AF-coupled ones. Contrary to the insistence on efficiency of AF-coupled free layers[4], we have obtained superior characteristics in the F-coupled free layers of very high thermal stability with keeping switching current density constant.

Acknowledgements

This work is partially supported by New Energy and Industrial Technology Development Organization (NEDO).

References

[1] S. Ikeda et al., IEEE Trans. Electron Devices 54, 991 (2007).
[2] T. Kishi et al., Electron Devices Meeting, 2008. IEDM 2008. IEEE International, 399 (2008).
[3] H. Kubota et al., Jpn. J. Appl. Phys. Part 2 44, L1237 (2005).
[4] J. Hayakawa et al., Jpn. J. Appl. Phys. Part 2 45, L1057 (2006).
[5] T. Kawahara et al., International Solid-State Circuits Conference, 2007. ISSCC Technical Digest. , 480 (2007).
[6] R. H. Koch, J. A. Katine, and J. Z. Sun, Phys. Rev. Lett. 92, 088302 (2004).

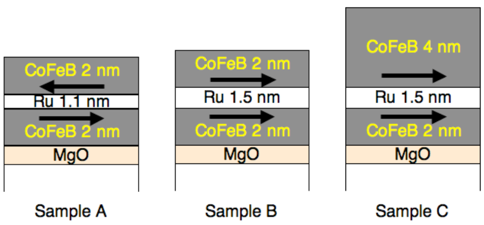

Fig. 1 Layer stacks of the coupled free layers. In the free layers, CoFeB layers are antiferromagnetically coupled in Sample A and ferromagnetically coupled in Sample B and C.

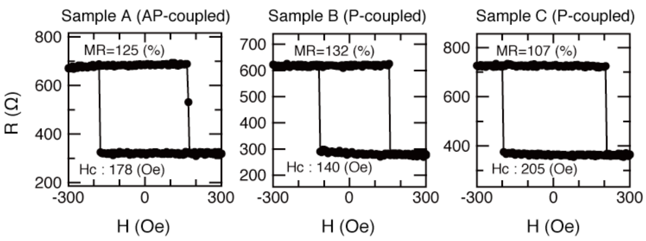

Fig. 2 Typical MR loops of the samples. Every sample shows a large MR ratio over 100% at RT.

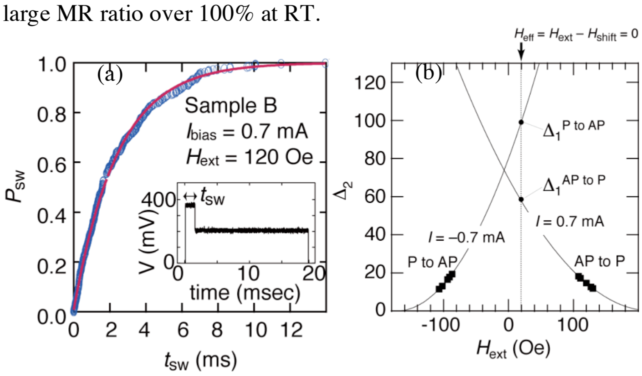

Fig. 3 Examples of spin-transfer switching measurement. (a) Switching probability as a function of switching time under a current and a magnetic field in Sample B. Circles and a line represent experiment and theoretical fit based on eq. (1) described in the text, respectively. The inset shows one shot of time domain measurement. (b) H_{ext} dependence of Δ_2 for the same sample. Squares and lines represent experiment and theoretical fit based on eq. (2), respectively. Δ_1 values for P to AP and AP to P switching are indicated in the figure.

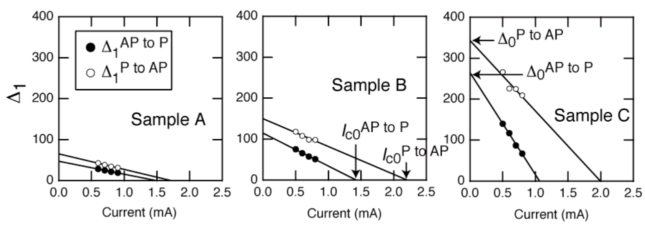

Fig. 4 Current bias dependence of Δ_1 in Sample A-C. Circles and lines represent experiment and theoretical fit based on eq. (3), respectively. The y- and x-intercepts represent Δ_0 and I_{c0} values, respectively.

Table 1 MR and the spin-transfer switching properties

	Sample A	Sample B	Sample C
Coupling	AF	F	F
MR (%)	121±7	128±3	103 ±3
J_{c0}^{ave}(MA/cm²)	18 ±2	19 ±1	19 ±2
Δ_0^{ave}	66 ±25	146 ±28	278 ±14
H_{c0}^{ave}(Oe)	313 ±12	218 ±36	290 ±30

$(\Delta_0^{ave}=(\Delta_0^{AP\ to\ P}+\Delta_0^{P\ to\ AP})/2,\quad H_{c0}^{ave}=(H_{c0}^{AP\ to\ P}+H_{c0}^{P\ to\ AP})/2)$